Nucleic Acids Research, 2024, **52**, D1253–D1264
https://doi.org/10.1093/nar/gkad1087
Advance access publication date: 20 November 2023
Database issue

DRMref: comprehensive reference map of drug resistance mechanisms in human cancer

Xiaona Liu[1], Jiahao Yi[2], Tina Li[1], Jianguo Wen[1], Kexin Huang[3], Jiajia Liu[1], Grant Wang[4], Pora Kim[1,*], Qianqian Song[5,*] and Xiaobo Zhou[1,*]

[1]Center for Computational Systems Medicine, McWilliams School of Biomedical Informatics, The University of Texas Health Science Center at Houston, Houston, TX 77030, USA
[2]Bioinformatics and Biomedical Big Data Mining Laboratory, Department of Medical Informatics, School of Big Health, Guizhou Medical University, Guiyang 550025, China
[3]West China Biomedical Big Data Centre, West China Hospital, Sichuan University, Chengdu, Sichuan 610041, China
[4]Department of Bioengineering, Rice University, Houston, TX 77005, USA
[5]Department of Health Outcomes and Biomedical Informatics, College of Medicine, University of Florida, Gainesville, FL 32610, USA

[*]To whom correspondence should be addressed. Tel: +1 713 500 3923/3636; Email: xiaobo.zhou@uth.tmc.edu
Correspondence may also be addressed to Qianqian Song. Tel: +1 352 627 9467; Email: qsong1@ufl.edu
Correspondence may also be addressed to Pora Kim. Tel: +1 713 500 3636; Email: Pora.Kim@uth.tmc.edu
Present address: Tina Li, Department of Statistics, Rice University, Houston, TX 77005, USA.

Abstract

Drug resistance poses a significant challenge in cancer treatment. Despite the initial effectiveness of therapies such as chemotherapy, targeted therapy and immunotherapy, many patients eventually develop resistance. To gain deep insights into the underlying mechanisms, single-cell profiling has been performed to interrogate drug resistance at cell level. Herein, we have built the DRMref database (https://ccsm.uth.edu/DRMref/) to provide comprehensive characterization of drug resistance using single-cell data from drug treatment settings. The current version of DRMref includes 42 single-cell datasets from 30 studies, covering 382 samples, 13 major cancer types, 26 cancer subtypes, 35 treatment regimens and 42 drugs. All datasets in DRMref are browsable and searchable, with detailed annotations provided. Meanwhile, DRMref includes analyses of cellular composition, intratumoral heterogeneity, epithelial–mesenchymal transition, cell–cell interaction and differentially expressed genes in resistant cells. Notably, DRMref investigates the drug resistance mechanisms (e.g. Aberration of Drug's Therapeutic Target, Drug Inactivation by Structure Modification, etc.) in resistant cells. Additional enrichment analysis of hallmark/KEGG (Kyoto Encyclopedia of Genes and Genomes)/GO (Gene Ontology) pathways, as well as the identification of microRNA, motif and transcription factors involved in resistant cells, is provided in DRMref for user's exploration. Overall, DRMref serves as a unique single-cell-based resource for studying drug resistance, drug combination therapy and discovering novel drug targets.

Graphical abstract

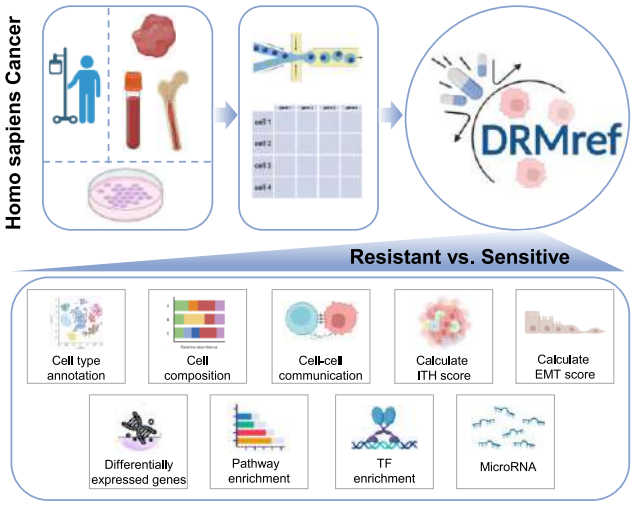

Received: August 15, 2023. **Revised:** October 18, 2023. **Editorial Decision:** October 28, 2023. **Accepted:** October 30, 2023

Introduction

Drug resistance has become a major concern in healthcare (1). For instance, a meta-analysis of 570 phase II single-agent clinical studies found that the median response rate to chemotherapy was only 11.9%. Even in the context of personalized targeted therapy, the response rate was as low as 30% (2). With the rapid development of sequencing technology, single-cell RNA sequencing (scRNA-seq) has become a revolutionary technique, enabling high-resolution investigations of tumor cell resistance at the cellular and cell type levels (3–12). For example, scRNA-seq analysis of prostate tumor tissue revealed that the activation of noncanonical Wnt signaling contributes to the cellular resistance of tumor cells against androgen receptor inhibitors (5). Another study profiled scRNA-seq of drug-resistant multiple myeloma samples and identified that peptidylprolyl isomerase A (PPIA), a key enzyme in the protein-folding response pathway, could serve as a potential novel target for resistant tumor cells (7). To overcome the ALK inhibitor-related resistance in lung cancer therapeutics, Heo *et al*. analyzed scRNA-seq data and identified cytidine deaminase as a potential druggable target to eliminate resistant cells (13). Those findings highlight the remarkable capability of scRNA-seq in exploiting the precise mechanisms underlying drug resistance, ultimately leading to the identification of effective targets and the development of optimized therapeutic strategies.

Currently, there are several drug-related databases available. For example, the DRESIS database collects validated drug resistance molecules belonging to different drug resistance mechanisms by retrieving published literature, and explicitly describes clinically/experimentally verified resistance data for a large number of drugs (14). The CTR-DB database utilizes pretreatment bulk RNA-seq data to characterize cancer drug response (15). CeDR Atlas is primarily based on scRNA-seq data to utilize the Connectivity Map resource for drug response prediction (16). CREAMMIST provides an integrative summary of the dose–response curve across datasets based on cancer cell line data (17). CancerDR is a resource encompassing 148 anticancer drugs and their pharmacological profiles across 952 cancer cell lines (18). GEAR presents genomic elements, including genes, single-nucleotide polymorphisms and microRNAs (miRNAs) that are associated with drug resistance via literature mining (19). KinaseMD mines the existing literature and provides annotations of mutations and their corresponding kinase inhibitor responses in four types of protein substructures that have been associated with kinase inhibitor resistance (20). However, there is still a lack of comprehensive characterization of drug resistance mechanisms using single-cell data obtained from drug treatment settings. To this end, we built the DRMref, a reference atlas of drug resistance mechanisms based on a collection of single-cell datasets, to elucidate resistance mechanisms across different cell types. Our database reveals the intricate landscape of drug resistance, facilitates a deep understanding of resistance complexity at single-cell level and aids in the development of improved therapeutic interventions.

To accomplish this, we annotated and analyzed 42 single-cell datasets with drug resistance information from 30 studies, 14 of which have both pre- and post-treatment samples, encompassing 26 cancer subtypes obtained from Gene Expression Omnibus (GEO) database and PubMed queries. These datasets are accompanied by crucial drug response information under three major drug categories: chemotherapy, targeted therapy and immunotherapy. For those single-cell datasets, we performed rigorous preprocessing steps, including quality control and the elimination of batch effects. We then identified resistance-related differentially expressed genes (R-DEGs) by comparing resistant cells with sensitive cells in each of the cell types. To gain insights into the drug resistance mechanisms of these R-DEGs, we conducted functional annotations using enrichment analysis, covering six well-known drug resistance mechanisms: 'Unusual Activation of Pro-survival Pathway', 'Irregularity in Drug Uptake and Drug Efflux', 'Aberration of the Drug's Therapeutic Target', 'Epigenetic Alteration of DNA, RNA or Protein', 'Drug Inactivation by Structure Modification' and 'Regulation by the Disease Microenvironment' (14). We also performed enrichment analysis on hallmark (21,22), KEGG (Kyoto Encyclopedia of Genes and Genomes) (23) and GO (Gene Ontology) (24) biological process (BP) pathways, as well as transcription factor (TF) and miRNA regulatory analysis, for a more in-depth annotation of R-DEGs. Moreover, to provide a deep understanding of the malignant cell activity, we compared intratumoral heterogeneity (ITH) and epithelial–mesenchymal transition (EMT) scores between the resistant and sensitive cells. Given that tumor microenvironment (TME) has been indicated to be associated with drug resistance, we further examined alterations in the TME during drug resistance by comparing the compositions of all cell types. In-depth analysis of cell–cell interactions was performed to investigate the impact of the surrounding microenvironment on cellular responses to drugs. As explained here, DRMref provides a comprehensive knowledge of drug resistance mechanisms.

Materials and methods

Data collection and preprocessing

First, we downloaded the Food and Drug Administration (FDA)-approved drug list (https://www.fda.gov/). To systematically collect scRNA-seq data, we searched previously published studies from PubMed by using the keyword '(drug name) AND ((single cell) OR (scRNA))' and '(drug resistance) AND ((single cell) OR (scRNA))'. Only samples from *Homo sapiens* with available drug response information were included. Overall, we collected 42 scRNA-seq datasets from 30 studies, 14 of which have both pre- and post-treatment samples, covering 382 samples, 13 major cancer types, 26 cancer subtypes, 35 treatment regimens and 42 drugs (Supplementary Table S1). According to the drug response information, cells of the nonresponsive samples collected from pre- or post-treatment conditions are labeled as resistant cells, while cells of the responsive samples are labeled as sensitive cells. The drug resistance information for each sample and each dataset is available in the 'Download' section of the DRMref database.

For scRNA-seq data preprocessing, cells with the number of expressed genes <500 and with the mitochondrial gene ratio $>10\%$ were excluded from most datasets. Datasets with batch effects were further processed using Harmony (25), which is a commonly used method to overcome bias within datasets from different sources. Detailed preprocessing steps for each dataset are provided in the 'Download' section of the DRMref database. All preprocessing was performed by Seurat 4.3.0 (26).

Cell clustering and annotation in scRNA-seq data

Cell clustering of scRNA-seq data was performed based on the normalized gene expression profile using the 'SCTransform' function of the Seurat package (26) in R. Cell type annotation was determined using totally 86 markers provided by the original and relevant studies (Supplementary Table S2). Uniform manifold approximation and projection (UMAP) was used to visualize the cell clusters, cell types and drug response (resistant and sensitive).

Alteration of cellular composition

We analyzed the changes in cell compositions between the resistant and sensitive cells utilizing scCODA 0.1.9 (27). This analysis was performed on datasets consisting of >3 resistant and sensitive samples. The pre- and post-treatment samples were analyzed separately, with the 'est_fdr' parameter set to 0.2.

Comparison of ITH and EMT scores of malignant cells

The ITH score was defined as the average Euclidean distance between each individual malignant cell and all other malignant cells, based on the first 20 principal components obtained from the normalized expression levels of highly variable genes (28). Here, the highly variable genes were identified by the 'SCTransform' function in the Seurat package with default parameters. The EMT score of malignant cells was calculated using the gsva function in the GSVA package (29), based on the 'Epithelial–Mesenchymal Transition' gene set obtained from the Molecular Signatures Database (MSigDB) (22). The difference in ITH scores and EMT scores between the resistant and sensitive cells was compared using the Wilcoxon test, and the results were visualized using violin plots.

Cell–cell interaction analysis

To identify the intercellular communications related to drug resistance, we performed cell–cell interaction analysis using CellPhoneDB (30), which is a publicly available repository of curated ligands, receptors and their interactions. Specifically, significant ligand–receptor interaction pairs were selected with a significant value of $P < 0.05$. The differences of cell–cell communications between the resistant and sensitive cells were visualized using heatmap, with numbers indicating the count of cell–cell interactions that were either higher or lower in resistant cells compared to sensitive cells. Additionally, dot plots were used to show the significant ligand–receptor pairs in resistant and sensitive cells, respectively.

Differential gene expression analysis for identifying drug resistance-related genes

We performed differential gene expression analysis between the resistant and sensitive cells for each cell type using the FindMarkers function in the Seurat package. The pre- and post-treatment samples were analyzed separately. DEGs with p_val_adj < 0.05 and $|avg\_log_2FC| > 0.25$ between the resistant and sensitive cells were considered drug resistance-related genes and are displayed in the database.

Mechanism analysis for drug resistance-related genes

To explore the potential resistance mechanisms of drug resistance-related genes (R-DEGs), we performed enrichment analysis of six known drug resistance mechanisms, hallmark, KEGG and GO BP pathways using hypeR 1.14.0 package (31) for upregulated genes and downregulated genes in each cell type, respectively. The hallmark, KEGG and GO BP gene sets are from the MSigDB (22). The pre- and post-treatment samples were analyzed separately. The gene set of six known drug resistance mechanisms was downloaded from DRESIS database. The enrichment results for the six known drug resistance mechanisms were not constrained by *P*-values. In the case of hallmark, KEGG and GO enrichment results, only the top 50 pathways with false discovery rate <0.05 were displayed.

Identifying miRNAs regulating drug resistance-related genes

The miRDB database (32) was utilized to predict miRNAs that regulate drug resistance-related genes (R-DEGs). miRNAs predicted to have scores exceeding 80 in the miRNA database were identified and can be downloaded from the 'Download' section. The miRNAs responsible for regulating the top 10 upregulated and downregulated genes in resistant malignant cells were shown by bubble plots.

Motif/TF enrichment analysis for drug resistance-related genes

Motif and TF enrichment analysis was performed using RcisTarget 1.18.2 package (33) based on the R-DEGs in each cell type. In the first step, RcisTarget selected DNA motifs that were significantly overrepresented in the surroundings of the transcription start site of the R-DEGs. This was achieved by utilizing a database containing genome-wide cross-species rankings for each motif. Subsequently, the motifs were annotated to TFs, and those with a high normalized enrichment score (NES) were retained. Motifs that passed the given threshold NES > 3.0 were considered significant. Finally, RcisTarget predicted the candidate target genes for each motif and gene set, i.e. genes within the gene set that are ranked above the leading edge.

Drug information

Drug information was extracted from DrugBank (version 5.1.10) (34). For each drug resistance-related gene, we examined whether it is a target of FDA-approved drugs.

Database architecture

The DRMref system is constructed based on a three-tier architecture: client, server and database. It includes a user-friendly web interface, a Perl's DBI module and a MySQL database. This database was developed in MySQL 3.23 with the MyISAM storage engine.

Results

Overview of DRMref

DRMref is a user-friendly and comprehensive database that utilizes scRNA-seq data to identify drug resistance-related molecular mechanisms across diverse cancer types, cell types

and drug categories in *H. sapiens* (Figure 1). scRNA-seq datasets from patient-derived clinical samples and *H. sapiens*-derived cell lines were manually collected and carefully curated from PubMed and GEO databases, along with the corresponding drug response information. The scRNA-seq data were downloaded and processed to a series of datasets, with each dataset including cells (resistant cells and sensitive cells) from the same therapeutic regimen and cancer subtype (with the finest granularity). If a certain dataset consists of cells at both pre- and post-treatment time points, analyses are done separately for cells at each time point.

Regarding each processed dataset, we performed cell composition analysis, ITH and EMT score analysis, cell communication analysis and differential gene expression analysis. Enrichment analysis based on six known drug resistance mechanisms and three existing biological pathway databases was performed. Further motif and TF enrichment analysis, as well as miRNA prediction, was done to provide deep insights of drug resistance in each cell type. All the results are accessible and viewable through each dataset's detailed annotation page. Given these in-depth analyses at single-cell level, our DRMref database will significantly enhance the understanding of drug resistance mechanisms. DRMref database will facilitate the identification of candidate predictive biomarkers, the exploration of diverse therapeutic approaches and the discovery of potential combination therapies to drug resistance.

The main functional modules of DRMref include 'Search' and 'Browse' (Figure 1). 'Search' supports gene and drug retrieval, through which detailed annotation pages of each gene and related datasets can be accessed. 'Browse' supports browsing cancer types, drug types and functional analyses, allowing access to detailed annotation pages of each dataset and drug resistance mechanisms. All analysis results can be downloaded and are presented through visually informative components such as heatmaps, bar plots, violin plots, dot plots, etc.

Data statistics of DRMref

In DRMref, we collected a total of 42 scRNA-seq datasets with drug resistance information from 30 studies, including 22 patient-derived datasets, 18 cell line-derived datasets, 1 PDX (patient-derived xenograft)-derived dataset and 1 CDX (cell line-derived xenograft)-derived dataset (Figure 2A). Among the patient-derived datasets, 14 of them contain both pre- and post-treatment samples. The DRMref database encompasses a total of 382 samples, covering 13 major cancer types, 26 cancer subtypes, 35 treatment regimens and 42 drugs spanning chemotherapy, targeted therapy and immunotherapy (Figure 2B). After quality control, we identified a total of 1 666 974 cells and 16 cell types based on 86 marker genes (Supplementary Table S2). Among them, 33 datasets included malignant cells (Figure 2C), with 13 datasets profiled from patients and 20 datasets from cell lines. Thirteen of the datasets comprised over 10 samples (Figure 2D). For most datasets, the average number of cells per sample ranges from 2000 to 8000 (Figure 2E). Based on the collected datasets, we identified 10 976 R-DEGs in total. Among them, 4076 R-DEGs were cancer type specific, 5107 R-DEGs were drug type specific and 3949 R-DEGs were cell type specific for a given cancer type. Among all the R-DEGs, 174 of them were TFs, 249 were oncogenes and 1670 were drug targets. Enrichment analysis for R-DEGs identified 50 significant hallmark pathways, 152 KEGG pathways and 4188 GO BP pathways. Mechanism analysis of R-DEGs identified a total of 636 genes that were enriched in six known drug resistance mechanisms. Motif/TF enrichment analysis identified 5127 unique enriched motifs/TFs with 8656 target genes. Among them, 174 TFs belong to R-DEGs. miRNA regulatory analysis identified 2617 enriched miRNAs with 8501 target genes.

DRMref search and browse

Users can perform searches by gene name (or ensemble name) and drug name (Figure 3A). When searching for a gene, the website will display datasets in which this gene is identified as the R-DEG, and users can access the detailed gene annotation page and dataset annotation page for this specific R-DEG. Clicking on a gene in the gene search table will redirect users to its detailed annotation page (Figure 3E). Meanwhile, clicking on the displayed datasets in the gene search table will redirect to the detailed functional analysis page of the dataset with this R-DEG (Figure 3F). Moreover, when searching for a drug, the website will display drug information and datasets related to that drug, and users can access the dataset analysis page (Figure 3F) for further exploration and analysis.

User can also browse by cancer type, drug type and functional analyses (Figure 3B–D), retrieve DRMref datasets and further access the detailed functional analysis results of each DRMref dataset (Figure 3F). The cancer type browse module displays 13 major cancer types, and the drug type browse module classifies drugs into three types (chemotherapy, targeted therapy and immunotherapy). Within the functional analyses browse module, each module displays datasets associated with that analysis. Additionally, the 'Enrichment analysis of six known drug resistance mechanisms' module also displays the R-DEGs enriched in six known drug resistance mechanisms. The 'Difference of cell–cell interactions between resistant and sensitive groups' module also shows the R-DEGs involved in significant ligand–receptor pairs. The 'Motifs and transcription factors (TFs) regulating drug resistance-related DEGs in each cell type' module also shows the R-DEGs belonging to enriched TFs. The 'Differentially expressed drug target genes between the resistant and sensitive groups' module also presents the R-DEGs that act as drug targets.

Exploration of DRMref features

Annotation of drug resistance-related genes

On the gene annotation page (Figure 3E), DRMref first provides the basic information of this gene. Then, DRMref displays the datasets with differential gene expression for this gene. Additionally, the dot plot was used to show the expression status of this gene across all datasets, time points and cell types, where red indicates high expression in the resistant cells, while blue indicates low expression in the resistant cells (Supplementary Figure S1). Moreover, the gene annotations mainly include significant ligand–receptor pairs, known drug resistance mechanisms, miRNA, motifs and TFs related to this gene. We also indicate whether this gene is a TF and drug target. Based on the identified important genes in resistant cells, our DRMref database can identify the important genes mentioned in the original research report. For instance, in the case of the GSE161195 dataset, the original article identified PPIA as a potential new target for overcoming drug resistance in the treatment of multiple myeloma following a combination therapy involving daratumumab, carfilzomib, lenalidomide and dexamethasone (7). DRMref also

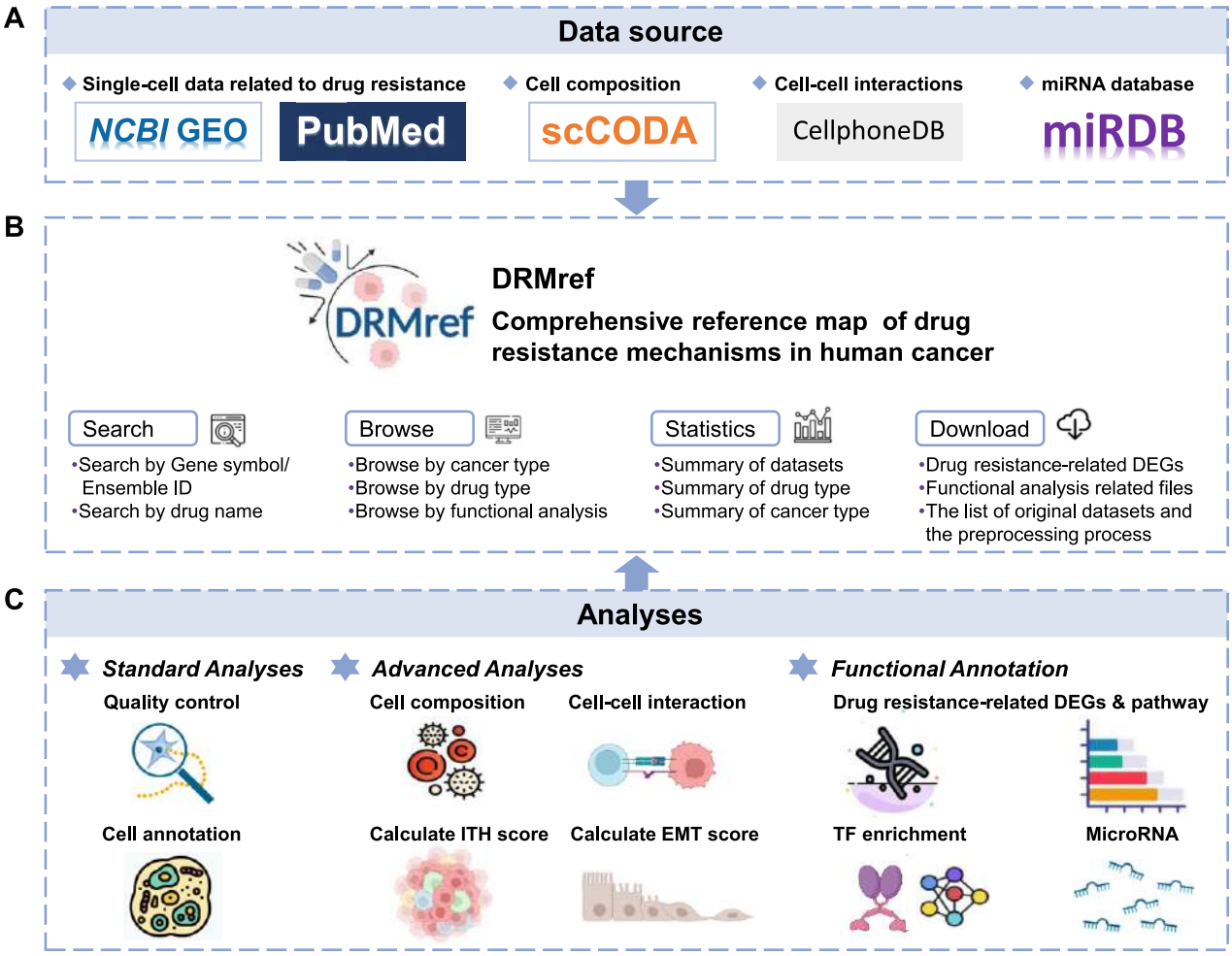

Figure 1. Overview of DRMref. (**A**) Public resources and analysis tools used in DRMref. (**B**) User interface of DRMref. (**C**) Comprehensive analyses in DRMref. The platform supports searching, browsing and downloading information, including drug resistance-related mechanisms and datasets.

identified PPIA as a significantly upregulated gene in the resistant cells. Furthermore, according to our DRMref results, we found that this gene is also significantly upregulated in other cancer types, such as post-treatment lung cancer and acute myeloid leukemia (GSE207422_Sin, GSE199333). Another example is the PMID34715028 dataset, which pertains to clear cell renal cell carcinoma. It reports an upregulation of GZMB expression in $CD8^+$ T cells from the group sensitive to nivolumab treatment (35). DRMref similarly identified a significant downregulation of GZMB expression in the resistant group. These results demonstrate that, with a uniform analytical workflow, DRMref not only uncovers critical information reported in the original studies, but also facilitates new knowledge insights.

Cell type module of dataset annotation

Based on the cell type markers (Supplementary Table S2), 16 major cell types were annotated in DRMref. This module provides visualization of cells with different cell types (Figure 4A), and different drug responses (resistant and sensitive; Supplementary Figure S2A). For cell line datasets, we also provide clustering visualizations of malignant cells, along with the proportions of cells with different drug responses within each cluster (Supplementary Figure S2B).

Cell composition module of dataset annotation

Since TME has been demonstrated to be associated with drug resistance, this module provides the statistical results of cell composition between the resistant and sensitive cells for both pre- and post-treatment samples (Figure 4B and Supplementary Figure S3). Immune cells play important roles in drug therapy and resistance (36–38). For example, natural killer (NK) cell therapy has been under research and has already undergone clinical trials (39). In DRMref, we consistently observed a significantly increased infiltration of NK cells in resistant samples of breast cancer post-treated with paclitaxel and endometrial cancer post-treated with pembrolizumab (Supplementary Figure S3A and B). However, B cells were shown as decreased in resistant samples of these two datasets (Supplementary Figure S3A and B). In contrast, for multiple myeloma treated with pomalidomide + dexamethasone or lenalidomide + dexamethasone, NK cells were notably reduced in the post-treatment resistant samples (Figure 4B and Supplementary Figure S3C). Meanwhile, other immune cells such as $CD4^+$ T cells, $CD8^+$ T cells and Mono/Macro cells also exhibited changes between resistant and sensitive conditions (Supplementary Figure S3C–F). These findings confirm the association between immune cell infiltration and the intricate development of drug resistance.

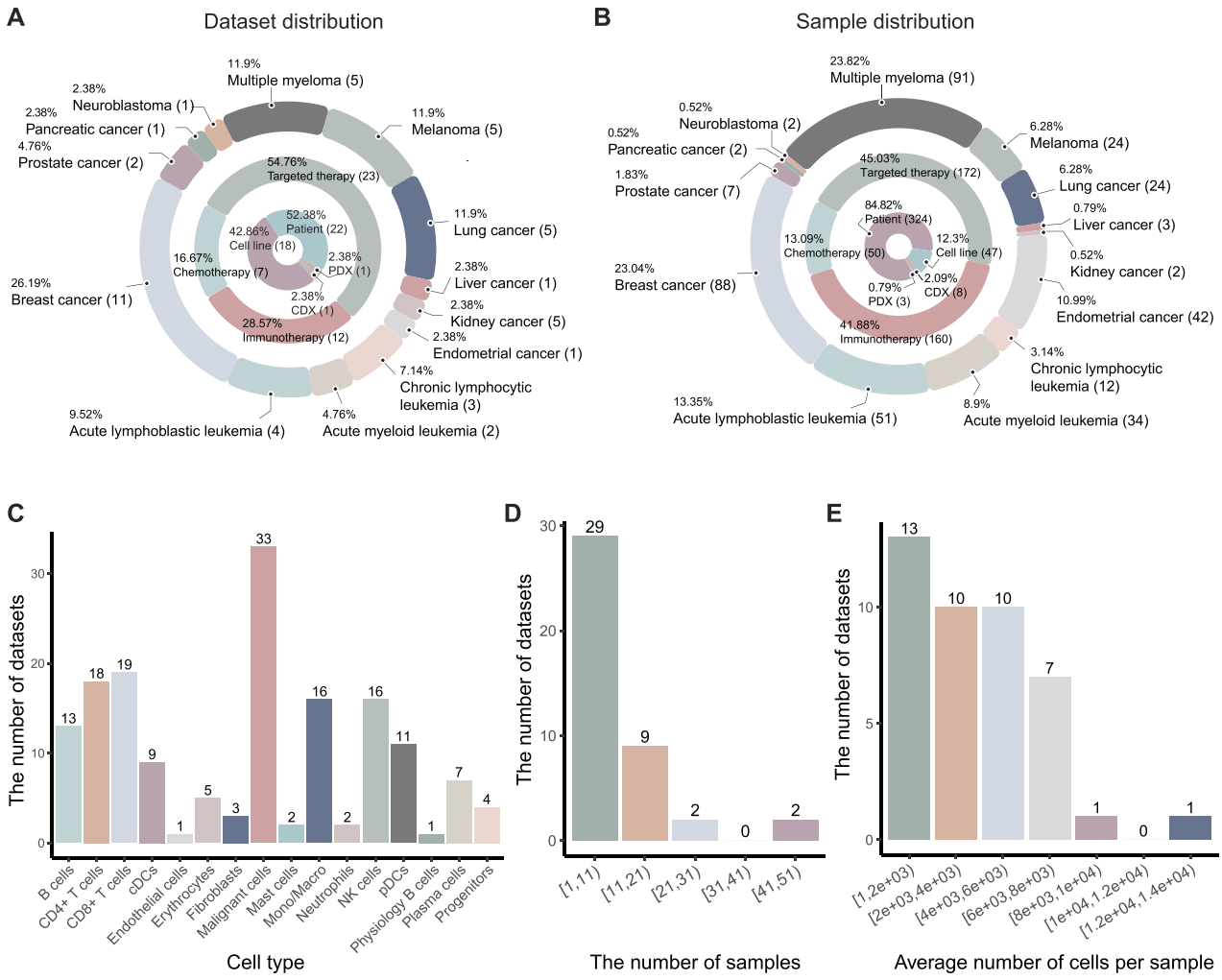

Figure 2. Data statistics of DRMref. (**A**) Dataset distribution of sample source, drug type and major cancer type. (**B**) Sample distribution regarding sample source, drug type and major cancer type. (**C**) The number of datasets on different cell types. (**D**) Statistics of sample sizes of datasets. (**E**) Statistics of average cell number of datasets.

ITH and EMT score module of dataset annotation

When tumor cells acquire drug resistance, ITH changes and EMT may occur. ITH describes the diversity of cell populations within a single tumor (40). ITH leads to a series of biological and host environmental changes, primarily through alterations in transcriptome expression and cell-to-cell interactions. Tumor heterogeneity itself and these changes contribute to drug resistance (41). EMT is a crucial cellular process that promotes metastasis in various tumors by causing the loss of an epithelial cell phenotype and by increasing or decreasing the expression of certain genes regulated by a small number of EMT TFs (42). EMT is also considered a key factor in drug resistance. Therefore, in this module, we analyzed the differences of ITH and EMT between the resistant malignant cells and sensitive malignant cells in both pre- and post-treatment samples (Supplementary Figure S4). As is known, ITH is closely related to treatment resistance and is described as the Rosetta Stone of therapy resistance (43,44). Previous studies have revealed increased ITH after the development of therapy resistance (45,46). Meanwhile, EMT, an important part of cell plasticity, is recognized as an important emerging factor in drug resistance (47,48). Many studies have reported the relationship between EMT and drug resistance in cancer (49,50). Consistent with these previous studies, we found that most tumors had larger ITH scores and EMT scores in the resistant cells compared to the sensitive cells.

Cell–cell communication module of dataset annotation

The cell–cell interaction is an important method to characterize the TME. It can induce the release of factors related to immune evasion and remodeling, further promoting the occurrence of treatment resistance (36). The interaction between cancer cells and nonmalignant cells within the TME often reshapes the environment and promotes drug resistance (51). Therefore, in order to delve deep into the impact of surrounding cells on malignant cell resistance, this module presents significant ligand–receptor interactions between different cell types in resistant and sensitive conditions. The analysis was conducted separately for pre- and post-treatment samples. The heatmap illustrates the changes in the number of significant ligand–receptor pairs in the resistant condition compared to the sensitive condition (Supplementary Figure S5A). The difference in the number of ligand–receptor pairs between the resistant and sensitive groups can indicate the

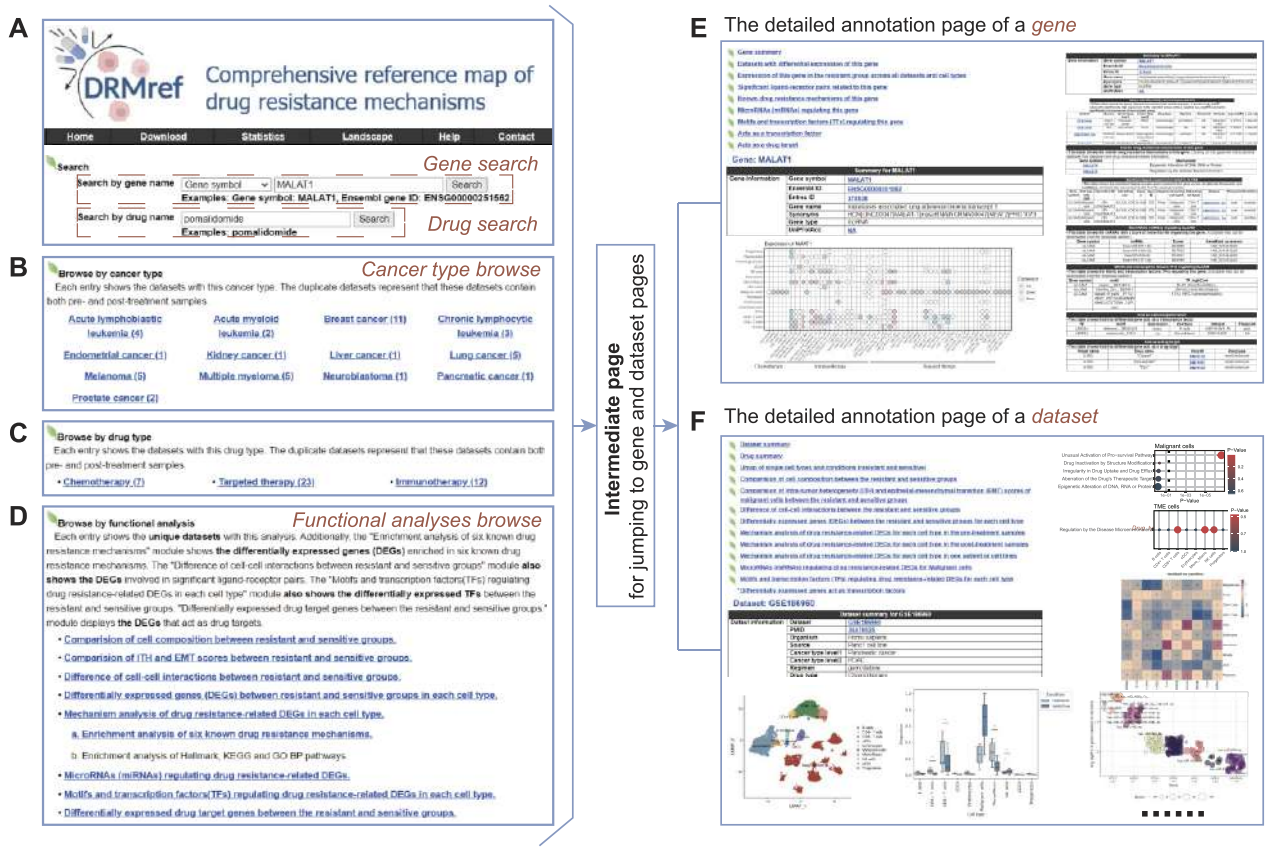

Figure 3. The 'Search' and 'Browse' modules of DRMref. (**A**) DRMref gene and drug search module. (i) Searching the gene symbol/ensemble gene ID will navigate to an intermediate page that includes datasets with this gene differentially expressed in resistant cells. (ii) Searching the drug name will navigate to an intermediate page showing drug information and datasets with this drug. (**B**) Cancer type browse module. (**C**) Drug type browse module. (**D**) Functional analyses browse module. (**E**) The detailed annotation page of an R-DEG. Clicking the gene name on the intermediate page will go to this page. (**F**) The detailed annotation page of a dataset. Clicking the dataset ID on the intermediate page will go to this page. R-DEG: drug resistance-related differentially expressed gene.

macroscopic changes in cell communication that occur under resistant conditions. The dot plots show the significant ligand–receptor pairs in the resistant and sensitive conditions, respectively (Figure 4C and Supplementary Figure S5B). Cell–cell communication analysis using scRNA-seq data identified totally 46 668 significant ligand–receptor pairs for different cancer types and drug categories. Among them, there were 604 unique pairs, with 198 of them associated with 115 R-DEGs. For example, our findings revealed that IGFBP3 was upregulated in resistant malignant cells of prostate cancer, breast cancer, lung cancer and melanoma, as well as in post-treatment samples of lung cancer treated with sintilimab (Supplementary Figure S1C). Notably, we identified IGFBP3–TMEM219 as a significant ligand–receptor pair between the resistant malignant cells and other cells in the TME of GSE207422_Sin dataset (Figure 4C). As we all know, IGFBP3 contributes to various human diseases through IGF/IGF-IR-independent actions (52–54). For example, the IGFBP3/TMEM219 axis holds significant clinical implications in cancer diagnosis and prognosis assessment (55,56). These results indicated that the altered interactions might be a potential mechanism of drug resistance.

Drug resistance-related DEG module of dataset annotation

Genes are the most fundamental factor in the study of drug resistance mechanisms and the basis for the analysis of downstream mechanisms. This module displays the significant DEGs between the resistant and sensitive cells (Supplementary Figure S6A). A total of 10 976 R-DEGs were identified across different datasets and cell types. By clicking on each gene, users can access its gene annotation page, which provides a series of information about the gene. For instance, metastasis-associated lung adenocarcinoma transcript 1 (MALAT1) was found as upregulated in resistant malignant cells across 17 datasets, encompassing 8 cancer types and 3 drug categories (Figure 4G). Meanwhile, MALAT1 was enriched in 'Epigenetic Alteration of DNA, RNA or Protein' and 'Regulation by the Disease Microenvironment' drug resistance mechanisms. As an evolutionary conserved long noncoding RNA, MALAT1 is known to regulate genes involved in cancer metastasis and cell migration (57), as well as drug resistance (58–60). For example, it can modulate the chemoresistance (cisplatin, adriamycin, gefitinib and paclitaxel) of non-small cell lung cancer (NSCLC) cells through regulating CTNND1 (61). CTNND1 is a key regulator of cell–cell adhesion (62,63) and is also shown upregulated in resistant cells (Supplementary Figure S1A), which indicate that the MALAT1–CTNND1 axis may serve as potential target to overcome NSCLC chemoresistance. Apart from MALAT1 and CTNND1, DRMref also provides other genes and functions that play crucial roles in drug resistance, demonstrating that our database can be utilized to interrogate novel targets for improved therapeutics.

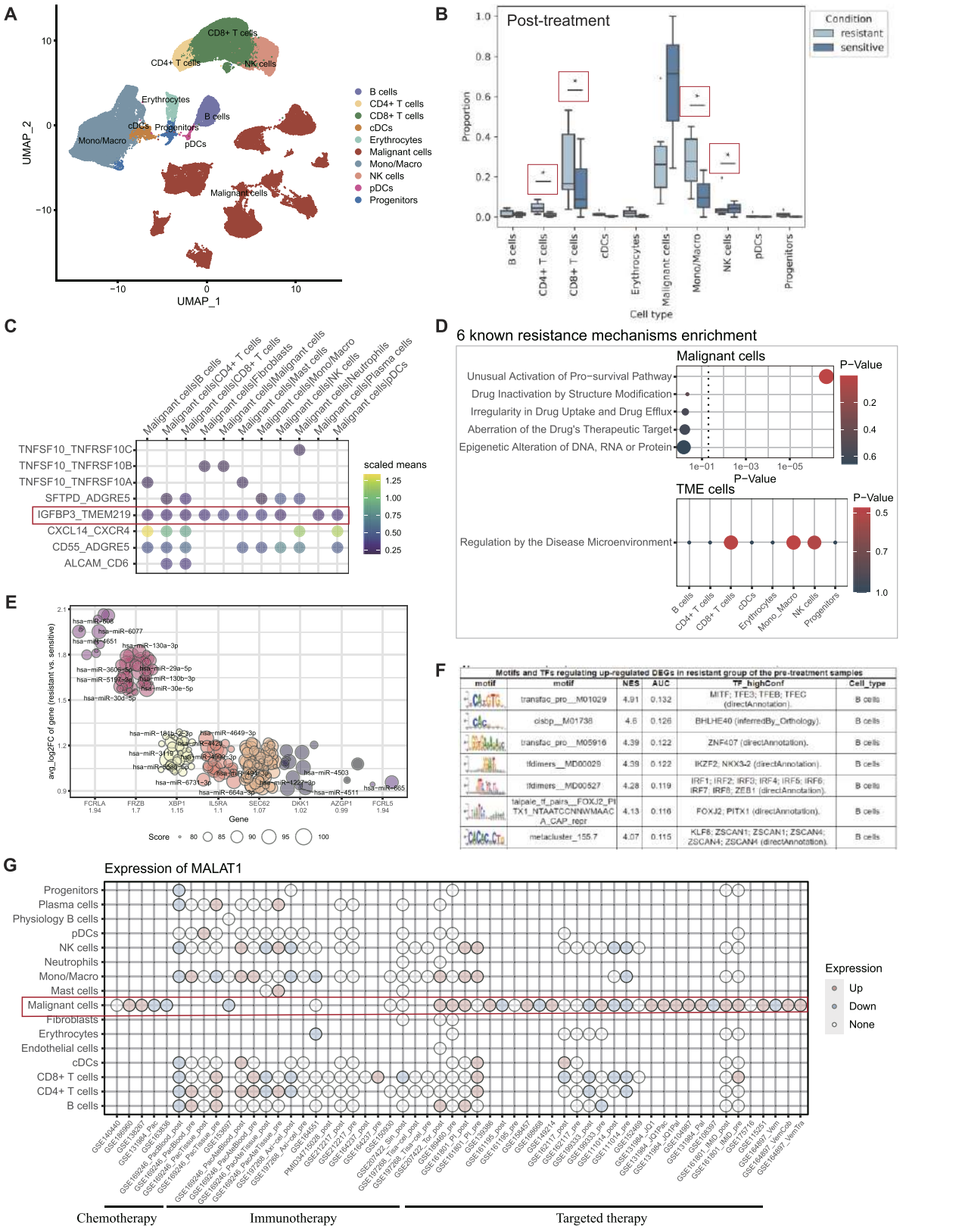

Figure 4. Example of dataset analysis results. (**A**) UMAP of cell types. If this dataset has both pre- and post-treatment samples, the cell types were annotated together. (**B**) The comparison of cell composition between the resistance and sensitive conditions at the post-treatment time point in the GSE161801_IMiD dataset. (**C**) The dot plot displays the partial significant ligand–receptor pairs between the malignant cells and the TME cells in the GSE207422_Sin dataset. (**D**) Enrichment results for five known drug resistance mechanisms in malignant cells and one known drug resistance mechanism in TME cells. (**E**) The bubble plot showed the top 10 upregulated genes in malignant cells along with their associated miRNAs with a prediction score of >80. (**F**) The list of motifs and TFs that regulate drug resistance-related DEGs for each cell type. (**G**) Expression of MALAT1 across all datasets and cell types.

Drug resistance mechanism module of dataset annotation

To interrogate the BPs linked with drug resistance, this module presents the enrichment analysis results of the six known drug resistance mechanisms (14) (Figure 4D) and biological pathways for the identified R-DEGs (Supplementary Figure S6B). DRMref also presents the gene list enriched in each drug resistance mechanism on the dataset annotation page. In total, 636 R-DEGs were found to be enriched in these six known drug resistance mechanisms. The functional characteristics of the R-DEGs were further delineated, including their involvement in KEGG pathways, hallmark gene sets and GO BP gene sets. These analyses aid in the discovery of candidate biological pathways that are crucial for drug resistance. Here, we identified a total of 50 significant hallmark gene sets, 152 KEGG pathways and 4188 GO BP gene sets. For each class of gene sets, a dot plot will be shown, presenting the top 50 upregulated gene sets and the top 50 downregulated gene sets, respectively.

miRNA module of dataset annotation

To better annotate the function of drug resistance-related genes, this section presents miRNAs related to R-DEGs. miRNAs predicted to have scores exceeding 80 in the miRDB database (32) were identified for each R-DEG. We identified 2617 enriched miRNAs that target 8501 R-DEGs. On the dataset annotation page, we showed the top 10 upregulated and top 10 downregulated R-DEGs in malignant cells along with their associated miRNAs using bubble plots, as shown in Figure 4E. Complete files containing all datasets and cell types can be downloaded from the 'Download' section.

Motif and TF enrichment module of dataset annotation

TFs play crucial roles in drug resistance. Accordingly, DRMref provides information on enriched motifs and TFs derived from R-DEGs in each cell type and dataset (Figure 4F). Additionally, as shown in Supplementary Figure S6C, we also provide the list of R-DEGs that act as TFs in this dataset. The motif/TF enrichment analysis identified 5127 unique enriched motifs/TFs associated with 8656 R-DEGs. Among them, 174 TFs are related to drug resistance. In our findings, SOX4 was found to be enriched as a TF in malignant cells, and it was upregulated in pancreatic cancer, lung cancer, breast cancer, acute myeloid leukemia and melanoma (Supplementary Figure S1B). As is known, SOX4 belongs to the SRY-related HMG box (SOX) TF family and is implicated in the development of various malignancies (64). Additionally, SOX4 was reported to induce drug resistance in colorectal cancer cells by downregulating CYLD through the transcriptional activation of miRNA-17 (65). These results demonstrate that our database provides in-depth information regarding motifs and TFs related to drug resistance.

Discussion

As an important topic in disease therapy, drug resistance has been addressed by several databases from different perspectives. However, DRMref is the first reference map of drug resistance mechanisms based on collections of single-cell data, characterizing drug resistance-related genes across diverse tissues and cell types in *H. sapiens*, along with related functional analyses. Functional analyses include ITH score and EMT score in malignant cells, cell composition analysis for showing the alteration of cell types between the resistant and sensitive conditions, cell–cell communication analysis for showing the alteration of significant ligand–receptor interactions, miRNA prediction, motif and TF enrichment analysis, and pathway enrichment analysis. Through DRMref, users can explore intercellular interactions using the expression profiling of ligands and receptors in the TME. DRMref also provides enrichment information for six known drug resistance-related mechanisms, allowing us to understand the known mechanisms of this drug in this type of cancer. Pathway enrichment analysis enables us to gain insights into the pathway changes that occur between resistance and sensitive cells. To date, DRMref has identified 10 976 resistance-related R-DEGs. Among them, 174 are TFs, 249 are oncogenes and 1670 are drug targets. Six hundred thirty-six genes are enriched in six known drug resistance mechanisms. Additionally, 115 resistance-related DEGs are associated with 198 significant ligand–receptor pairs.

Meanwhile, under different methods or parameters, or when compared to the results from the original article, the results of the DRMref database demonstrate a high degree of consistency. As shown in Supplementary Figure S7, in the GSE161801_IMiD dataset, the overlap rate of six cell types with the annotations in the original article is almost above 90%. In the GSE161801_PI dataset, the overlap rate for four cell types is also nearly above 90%. In the DRMref database's GSE169246_PacAteBlood dataset, there are 111 overlapping DEGs with the original article, accounting for 90.24% of the DEGs reported in the original article. Moreover, the DRMref database not only identified key genes, as highlighted in the original articles, but also facilitated the discovery of new insights by using this universal workflow and integrated datasets. Therefore, the results of the DRMref database are reliable and meaningful.

In order to maintain DRMref as a cutting-edge drug resistance database, we will continuously collect and update new data every 6 months. Additionally, we welcome users to share publicly available drug resistance scRNA-seq data on our website. We will employ advanced modeling methods and deep learning-based transformation techniques to extract valuable insights from our database, enabling combination analysis for investigating drug combinations and identifying targetable biomarkers. This will facilitate the development of enhanced therapeutics, research on drug resistance mechanisms, and the discovery of combinational biomarkers, drug response predictions and clinical drug recommendations. We firmly believe that DRMref will continue to serve as a valuable resource for drug resistance research and drug target discovery.

Data availability

All data and results can be downloaded from the DRMref website (https://ccsm.uth.edu/DRMref/).

Supplementary data

Supplementary Data are available at NAR Online.

Acknowledgements

We extend our heartfelt gratitude to all our colleagues, friends and IT team who offered valuable advice and support during the course of this study. Our sincere appreciation also goes to the generous researchers who selflessly shared their data.

Authors contributions: Xiaona Liu contributed to the conception and design, data acquisition, analysis, and interpretation, and drafted the work. Jiahao Yi contributed to data acquisition, analysis, and drafting of the work. Tina Li contributed to data acquisition, analysis, and drafting of the work. Jianguo Wen contributed to the conception and design of the work and critically revised the work for important intellectual content. Kexin Huang contributed to data interpretation and critically revised the work for important intellectual content. Jiajia Liu provided the basic code for website construction, helped modify the code, and contributed to some of the analysis work. Grant Wang contributed to the revision of important content and some of the analysis work. Pora Kim, Qianqian Song, and Xiaobo Zhou contributed to the conception and design, data interpretation of the work, and critically revised the work for important intellectual content. All authors provided their final approval for the version to be published and agreed to be accountable for all aspects of the work.

Funding

National Institutes of Health [R01GM123037, U01AR0 69395 and R01CA241930]; National Science Foundation [2217515 and 2326879]; National Institute of General Medical Sciences [R35GM151089 to Q.S., R35GM138184 to P.K.].

Conflict of interest statement

None declared.

References

1. Ward,R.A., Fawell,S., Floc'h,N., Flemington,V., McKerrecher,D. and Smith,P.D. (2021) Challenges and opportunities in cancer drug resistance. *Chem. Rev.*, **121**, 3297–3351.
2. Schwaederle,M., Zhao,M., Lee,J.J., Eggermont,A.M., Schilsky,R.L., Mendelsohn,J., Lazar,V. and Kurzrock,R. (2015) Impact of precision medicine in diverse cancers: a meta-analysis of phase II clinical trials. *J. Clin. Oncol.*, **33**, 3817–3825.
3. Tang,F., Barbacioru,C., Wang,Y., Nordman,E., Lee,C., Xu,N., Wang,X., Bodeau,J., Tuch,B.B., Siddiqui,A., *et al.* (2009) mRNA-seq whole-transcriptome analysis of a single cell. *Nat. Methods*, **6**, 377–382.
4. Jovic,D., Liang,X., Zeng,H., Lin,L., Xu,F. and Luo,Y. (2022) Single-cell RNA sequencing technologies and applications: a brief overview. *Clin. Transl. Med.*, **12**, e694.
5. Miyamoto,D.T., Zheng,Y., Wittner,B.S., Lee,R.J., Zhu,H., Broderick,K.T., Desai,R., Fox,D.B., Brannigan,B.W., Trautwein,J., *et al.* (2015) RNA-seq of single prostate CTCs implicates noncanonical Wnt signaling in antiandrogen resistance. *Science*, **349**, 1351–1356.
6. Li,W., Zhang,B., Cao,W., Zhang,W., Li,T., Liu,L., Xu,L., Gao,F., Wang,Y., Wang,F., *et al.* (2023) Identification of potential resistance mechanisms and therapeutic targets for the relapse of BCMA CAR-T therapy in relapsed/refractory multiple myeloma through single-cell sequencing. *Exp. Hematol.*, **12**, 44.
7. Cohen,Y.C., Zada,M., Wang,S.Y., Bornstein,C., David,E., Moshe,A., Li,B., Shlomi-Loubaton,S., Gatt,M.E., Gur,C., *et al.* (2021) Identification of resistance pathways and therapeutic targets in relapsed multiple myeloma patients through single-cell sequencing. *Nat. Med.*, **27**, 491–503.
8. Hinohara,K., Wu,H.J., Sébastien,V., McDonald,T.O., Igarashi,K.J., Yamamoto,K.N., Madsen,T., Fassl,A., Egri,S.B., Papanastasiou,M., *et al.* (2019) KDM5 histone demethylase activity links cellular transcriptomic heterogeneity to therapeutic resistance. *Cancer Cell*, **35**, 330–332.
9. Ding,X., Zhu,Z., Lapek,J., McMillan,E.A., Zhang,A., Chung,C.Y., Dubbury,S., Lapira,J., Firdaus,S., Kang,X., *et al.* (2022) PARP1–SNAI2 transcription axis drives resistance to PARP inhibitor, talazoparib. *Sci. Rep.*, **12**, 12501.
10. Samur,M.K., Fulciniti,M., Aktas Samur,A., Bazarbachi,A.H., Tai,Y.T., Prabhala,R., Alonso,A., Sperling,A.S., Campbell,T., Petrocca,F., *et al.* (2021) Biallelic loss of BCMA as a resistance mechanism to CAR T cell therapy in a patient with multiple myeloma. *Nat. Commun.*, **12**, 868.
11. Paulson,K.G., Voillet,V., McAfee,M.S., Hunter,D.S., Wagener,F.D., Perdicchio,M., Valente,W.J., Koelle,S.J., Church,C.D., Vandeven,N., *et al.* (2018) Acquired cancer resistance to combination immunotherapy from transcriptional loss of class I HLA. *Nat. Commun.*, **9**, 3868.
12. Sharma,A., Cao,E.Y., Kumar,V., Zhang,X., Leong,H.S., Wong,A.M.L., Ramakrishnan,N., Hakimullah,M., Teo,H.M.V., Chong,F.T., *et al.* (2018) Longitudinal single-cell RNA sequencing of patient-derived primary cells reveals drug-induced infidelity in stem cell hierarchy. *Nat. Commun.*, **9**, 4931.
13. Heo,H., Kim,J.H., Lim,H.J., Kim,J.H., Kim,M., Koh,J., Im,J.Y., Kim,B.K., Won,M., Park,J.H., *et al.* (2022) DNA methylome and single-cell transcriptome analyses reveal CDA as a potential druggable target for ALK inhibitor-resistant lung cancer therapy. *Exp. Mol. Med.*, **54**, 1236–1249.
14. Sun,X., Zhang,Y., Li,H., Zhou,Y., Shi,S., Chen,Z., He,X., Zhang,H., Li,F., Yin,J., *et al.* (2023) DRESIS: the first comprehensive landscape of drug resistance information. *Nucleic Acids Res.*, **51**, D1263–D1275.
15. Liu,Z., Liu,J., Liu,X., Wang,X., Xie,Q., Zhang,X., Kong,X., He,M., Yang,Y., Deng,X., *et al.* (2022) CTR-DB, an omnibus for patient-derived gene expression signatures correlated with cancer drug response. *Nucleic Acids Res.*, **50**, D1184–D1199.
16. Wang,Y.Y., Kang,H., Xu,T., Hao,L., Bao,Y. and Jia,P. (2022) CeDR Atlas: a knowledgebase of cellular drug response. *Nucleic Acids Res.*, **50**, D1164–D1171.
17. Yingtaweesittikul,H., Wu,J., Mongia,A., Peres,R., Ko,K., Nagarajan,N. and Suphavilai,C. (2023) CREAMMIST: an integrative probabilistic database for cancer drug response prediction. *Nucleic Acids Res.*, **51**, D1242–D1248.
18. Kumar,R., Chaudhary,K., Gupta,S., Singh,H., Kumar,S., Gautam,A., Kapoor,P. and Raghava,G.P. (2013) CancerDR: cancer drug resistance database. *Sci. Rep.*, **3**, 1445.
19. Wang,Y.Y., Chen,W.H., Xiao,P.P., Xie,W.B., Luo,Q., Bork,P. and Zhao,X.M. (2017) GEAR: a database of genomic elements associated with drug resistance. *Sci. Rep.*, **7**, 44085.
20. Hu,R., Xu,H., Jia,P. and Zhao,Z. (2021) KinaseMD: kinase mutations and drug response database. *Nucleic Acids Res.*, **49**, D552–D561.
21. Liberzon,A., Birger,C., Thorvaldsdóttir,H., Ghandi,M., Mesirov,J.P. and Tamayo,P. (2015) The Molecular Signatures Database (MSigDB) hallmark gene set collection. *Cell Syst.*, **1**, 417–425.
22. Subramanian,A., Tamayo,P., Mootha,V.K., Mukherjee,S., Ebert,B.L., Gillette,M.A., Paulovich,A., Pomeroy,S.L., Golub,T.R., Lander,E.S., *et al.* (2005) Gene set enrichment analysis: a knowledge-based approach for interpreting genome-wide expression profiles. *Proc. Natl Acad. Sci. U.S.A.*, **102**, 15545–15550.
23. Kanehisa,M. and Goto,S. (2000) KEGG: Kyoto Encyclopedia of Genes and Genomes. *Nucleic Acids Res.*, **28**, 27–30.
24. Ashburner,M., Ball,C.A., Blake,J.A., Botstein,D., Butler,H., Cherry,J.M., Davis,A.P., Dolinski,K., Dwight,S.S., Eppig,J.T., *et al.* (2000) Gene Ontology: tool for the unification of biology. The Gene Ontology Consortium. *Nat. Genet.*, **25**, 25–29.
25. Korsunsky,I., Millard,N., Fan,J., Slowikowski,K., Zhang,F., Wei,K., Baglaenko,Y., Brenner,M., Loh,P.R. and Raychaudhuri,S. (2019)

Fast, sensitive and accurate integration of single-cell data with Harmony. *Nat. Methods*, **16**, 1289–1296.
26. Hao,Y., Hao,S., Andersen-Nissen,E., Mauck,W.M. 3rd, Zheng,S., Butler,A., Lee,M.J., Wilk,A.J., Darby,C., Zager,M., *et al.* (2021) Integrated analysis of multimodal single-cell data. *Cell*, **184**, 3573–3587.
27. Büttner,M., Ostner,J., Müller,C.L., Theis,F.J. and Schubert,B. (2021) scCODA is a Bayesian model for compositional single-cell data analysis. *Nat. Commun.*, **12**, 6876.
28. Hu,X.E., Yang,P., Chen,S., Wei,G., Yuan,L., Yang,Z., Gong,L., He,L., Yang,L., Peng,S., *et al.* (2023) Clinical and biological heterogeneities in triple-negative breast cancer reveals a non-negligible role of HER2-low. *Breast Cancer Res.*, **25**, 34.
29. Hänzelmann,S., Castelo,R. and Guinney,J. (2013) GSVA: gene set variation analysis for microarray and RNA-seq data. *BMC Bioinformatics*, **14**, 7.
30. Efremova,M., Vento-Tormo,M., Teichmann,S.A. and Vento-Tormo,R. (2020) CellPhoneDB: inferring cell–cell communication from combined expression of multi-subunit ligand–receptor complexes. *Nat. Protoc.*, **15**, 1484–1506.
31. Federico,A. and Monti,S. (2020) hypeR: an R package for geneset enrichment workflows. *Bioinformatics*, **36**, 1307–1308.
32. Chen,Y. and Wang,X. (2020) miRDB: an online database for prediction of functional microRNA targets. *Nucleic Acids Res.*, **48**, D127–D131.
33. Aibar,S., González-Blas,C.B., Moerman,T., Huynh-Thu,V.A., Imrichova,H., Hulselmans,G., Rambow,F., Marine,J.C., Geurts,P., Aerts,J., *et al.* (2017) SCENIC: single-cell regulatory network inference and clustering. *Nat. Methods*, **14**, 1083–1086.
34. Wishart,D.S., Feunang,Y.D., Guo,A.C., Lo,E.J., Marcu,A., Grant,J.R., Sajed,T., Johnson,D., Li,C., Sayeeda,Z., *et al.* (2018) DrugBank 5.0: a major update to the DrugBank database for 2018. *Nucleic Acids Res.*, **46**, D1074–D1082.
35. Au,L., Hatipoglu,E., Robert de Massy,M., Litchfield,K., Beattie,G., Rowan,A., Schnidrig,D., Thompson,R., Byrne,F., Horswell,S., *et al.* (2021) Determinants of anti-PD-1 response and resistance in clear cell renal cell carcinoma. *Cancer Cell*, **39**, 1497–1518.
36. Khalaf,K., Hana,D., Chou,J.T., Singh,C., Mackiewicz,A. and Kaczmarek,M. (2021) Aspects of the tumor microenvironment involved in immune resistance and drug resistance. *Front. Immunol.*, **12**, 656364.
37. Li,C., Phoon,Y.P., Karlinsey,K., Tian,Y.F., Thapaliya,S., Thongkum,A., Qu,L., Matz,A.J., Cameron,M., Cameron,C., *et al.* (2022) A high OXPHOS CD8 T cell subset is predictive of immunotherapy resistance in melanoma patients. *J. Exp. Med.*, **219**, e20202084.
38. Bu,L., Baba,H., Yasuda,T., Uchihara,T. and Ishimoto,T. (2020) Functional diversity of cancer-associated fibroblasts in modulating drug resistance. *Cancer Sci.*, **111**, 3468–3477.
39. Chu,J., Gao,F., Yan,M., Zhao,S., Yan,Z., Shi,B. and Liu,Y. (2022) Natural killer cells: a promising immunotherapy for cancer. *J. Transl. Med.*, **20**, 240.
40. Sun,X.X. and Yu,Q. (2015) Intra-tumor heterogeneity of cancer cells and its implications for cancer treatment. *Acta Pharmacol. Sin.*, **36**, 1219–1227.
41. Zhang,A., Miao,K., Sun,H. and Deng,C.X. (2022) Tumor heterogeneity reshapes the tumor microenvironment to influence drug resistance. *Int. J. Biol. Sci.*, **18**, 3019–3033.
42. Yilmaz,M. and Christofori,G. (2009) EMT, the cytoskeleton, and cancer cell invasion. *Cancer Metastasis Rev.*, **28**, 15–33.
43. Marusyk,A., Janiszewska,M. and Polyak,K. (2020) Intratumor heterogeneity: the Rosetta Stone of therapy resistance. *Cancer Cell*, **37**, 471–484.
44. Lim,Z.F. and Ma,P.C. (2019) Emerging insights of tumor heterogeneity and drug resistance mechanisms in lung cancer targeted therapy. *J. Hematol. Oncol.*, **12**, 134.
45. Stewart,C.A., Gay,C.M., Xi,Y., Sivajothi,S., Sivakamasundari,V., Fujimoto,J., Bolisetty,M., Hartsfield,P.M., Balasubramaniyan,V., Chalishazar,M.D., *et al.* (2020) Single-cell analyses reveal increased intratumoral heterogeneity after the onset of therapy resistance in small-cell lung cancer. *Nat. Cancer*, **1**, 423–436.
46. Zhao,Y., Li,Z.X., Zhu,Y.J., Fu,J., Zhao,X.F., Zhang,Y.N., Wang,S., Wu,J.M., Wang,K.T., Wu,R., *et al.* (2021) Single-cell transcriptome analysis uncovers intratumoral heterogeneity and underlying mechanisms for drug resistance in hepatobiliary tumor organoids. *Adv. Sci.*, **8**, e2003897.
47. Du,B. and Shim,J.S. (2016) Targeting epithelial–mesenchymal transition (EMT) to overcome drug resistance in cancer. *Molecules*, **21**, 965.
48. De Las Rivas,J., Brozovic,A., Izraely,S., Casas-Pais,A., Witz,I.P. and Figueroa,A. (2021) Cancer drug resistance induced by EMT: novel therapeutic strategies. *Arch. Toxicol.*, **95**, 2279–2297.
49. Huang,J., Li,H. and Ren,G. (2015) Epithelial–mesenchymal transition and drug resistance in breast cancer (Review). *Int. J. Oncol.*, **47**, 840–848.
50. Nurwidya,F., Takahashi,F., Murakami,A. and Takahashi,K. (2012) Epithelial–mesenchymal transition in drug resistance and metastasis of lung cancer. *Cancer Res. Treat.*, **44**, 151–156.
51. Ni,Y., Zhou,X., Yang,J., Shi,H., Li,H., Zhao,X. and Ma,X. (2021) The role of tumor–stroma interactions in drug resistance within tumor microenvironment. *Front. Cell Dev. Biol.*, **9**, 637675.
52. Arab,J.P., Cabrera,D., Sehrawat,T.S., Jalan-Sakrikar,N., Verma,V.K., Simonetto,D., Cao,S., Yaqoob,U., Leon,J., Freire,M., *et al.* (2020) Hepatic stellate cell activation promotes alcohol-induced steatohepatitis through Igfbp3 and SerpinA12. *J. Hepatol.*, **73**, 149–160.
53. Min,H.K., Maruyama,H., Jang,B.K., Shimada,M., Mirshahi,F., Ren,S., Oh,Y., Puri,P. and Sanyal,A.J. (2016) Suppression of IGF binding protein-3 by palmitate promotes hepatic inflammatory responses. *FASEB J.*, **30**, 4071–4082.
54. Mehta,H.H., Gao,Q., Galet,C., Paharkova,V., Wan,J., Said,J., Sohn,J.J., Lawson,G., Cohen,P., Cobb,L.J., *et al.* (2011) IGFBP-3 is a metastasis suppression gene in prostate cancer. *Cancer Res.*, **71**, 5154–5163.
55. Cai,Q., Dozmorov,M. and Oh,Y. (2020) IGFBP-3/IGFBP-3 receptor system as an anti-tumor and anti-metastatic signaling in cancer. *Cells*, **9**, 1261.
56. Ingermann,A.R., Yang,Y.F., Han,J., Mikami,A., Garza,A.E., Mohanraj,L., Fan,L., Idowu,M., Ware,J.L., Kim,H.S., *et al.* (2010) Identification of a novel cell death receptor mediating IGFBP-3-induced anti-tumor effects in breast and prostate cancer. *J. Biol. Chem.*, **285**, 30233–30246.
57. Amodio,N., Raimondi,L., Juli,G., Stamato,M.A., Caracciolo,D., Tagliaferri,P. and Tassone,P. (2018) MALAT1: a druggable long non-coding RNA for targeted anti-cancer approaches. *J. Hematol. Oncol.*, **11**, 63.
58. Xi,Z., Si,J. and Nan,J. (2019) LncRNA MALAT1 potentiates autophagy-associated cisplatin resistance by regulating the microRNA-30b/autophagy-related gene 5 axis in gastric cancer. *Int. J. Oncol.*, **54**, 239–248.
59. YiRen,H., YingCong,Y., Sunwu,Y., Keqin,L., Xiaochun,T., Senrui,C., Ende,C., XiZhou,L. and Yanfan,C. (2017) Long noncoding RNA MALAT1 regulates autophagy associated chemoresistance via miR-23b-3p sequestration in gastric cancer. *Mol. Cancer*, **16**, 174.
60. Xia,C., Liang,S., He,Z., Zhu,X., Chen,R. and Chen,J. (2018) Metformin, a first-line drug for type 2 diabetes mellitus, disrupts the MALAT1/miR-142-3p sponge to decrease invasion and migration in cervical cancer cells. *Eur. J. Pharmacol.*, **830**, 59–67.
61. Yang,T., Li,H., Chen,T., Ren,H., Shi,P. and Chen,M. (2019) LncRNA MALAT1 depressed chemo-sensitivity of NSCLC cells through directly functioning on miR-197-3p/p120 catenin axis. *Mol. Cells*, **42**, 270–283.
62. Alharatani,R., Ververi,A., Beleza-Meireles,A., Ji,W., Mis,E., Patterson,Q.T., Griffin,J.N., Bhujel,N., Chang,C.A., Dixit,A., *et al.* (2020) Novel truncating mutations in CTNND1 cause a dominant craniofacial and cardiac syndrome. *Hum. Mol. Genet.*, **29**, 1900–1921.

63. Davis,M.A., Ireton,R.C. and Reynolds,A.B. (2003) A core function for p120-catenin in cadherin turnover. *J. Cell Biol.*, **163**, 525–534.
64. Wang,C., Zhao,H., Lu,J., Yin,J., Zang,L., Song,N., Dong,R., Wu,T. and Du,X. (2012) Clinicopathological significance of SOX4 expression in primary gallbladder carcinoma. *Diagn. Pathol.*, **7**, 41.
65. Pan,S., Bao,D., Li,Y., Liu,D., Quan,S. and Wang,R. (2022) SOX4 induces drug resistance of colorectal cancer cells by downregulating CYLD through transcriptional activation of microRNA-17. *J. Biochem. Mol. Toxicol.*, **36**, e22910.

Received: August 15, 2023. **Revised:** October 18, 2023. **Editorial Decision:** October 28, 2023. **Accepted:** October 30, 2023